

Chiral-extended photon-emitter dressed states in non-Hermitian topological baths

Zhao-Fan Cai,^{1,*} Xin Wang^{2,*} Zi-Xuan Liang,¹ Tao Liu^{1,†} and Franco Nori^{3,4}

¹*School of Physics and Optoelectronics, South China University of Technology, Guangzhou 510640, China*

²*Institute of Theoretical Physics, School of Physics, Xi'an Jiaotong University, Xi'an 710049, China*

³*Center for Quantum Computing, RIKEN, Wakoshi, Saitama 351-0198, Japan*

⁴*Department of Physics, University of Michigan, Ann Arbor, Michigan 48109-1040, USA*



(Received 20 August 2024; accepted 29 May 2025; published 10 June 2025)

The interplay of quantum emitters and non-Hermitian structured baths has received increasing attention in recent years. Here we predict unconventional quantum optical behaviors of quantum emitters coupled to a non-Hermitian topological bath, which is realized in a 1D Su-Schrieffer-Heeger photonic chain subjected to nonlocal dissipation. In addition to the Hermitian-like chiral bound states in the middle line gap and skin-mode-like hidden bound states inside the point gap, we identify peculiar in-gap chiral and extended photon-emitter dressed states. This is due to the competition of topological-edge localization and non-Hermitian skin-mode localization in combination with the non-Bloch bulk-boundary correspondence. Strikingly, dissipation can shape the wavefunction profile of the dressed state. Furthermore, when two emitters are coupled to the same bath, such in-gap dressed states can mediate the nonreciprocal long-range emitter-emitter interactions, with the interaction range limited only by the dissipation of the bath. Our work opens the door to further study rich quantum optical phenomena and exotic many-body physics utilizing quantum emitters coupled to non-Hermitian baths.

DOI: [10.1103/8qpx-68x6](https://doi.org/10.1103/8qpx-68x6)

Introduction. Recent years have witnessed considerable interest in controlling photon-emitter interactions utilizing structured nanophotonic environments due to their potential applications in quantum networks and quantum simulation of many-body physics [1–26]. Among them, one of the promising strategies is to couple quantum emitters with topological wave guides [7–16], where the topological nature of the bath can give rise to unconventional quantum optical phenomena robustness against disorder, e.g., chiral photon-emitter bound states, band topology-dependent super/subradiant states, and exotic many-body phases resulting from the tunable emitter-emitter interactions mediated by the bound states [12].

A photonic structure is unavoidably coupled to the external reservoir, which can be effectively described by non-Hermitian Hamiltonians [27]. Non-Hermitian physics is currently a burgeoning field due to the unique physical phenomenon without Hermitian counterparts [27–72]. An intriguing physical phenomenon is the non-Hermitian skin effect (NHSE), with the emergence of localized bulk modes at boundaries [37–42], which has the intrinsic topological origin associated to the point gap [50,55]. In recent years, the interplay of quantum emitters and non-Hermitian structured baths has attracted much attention [73–78], leading to exotic quantum optical behaviors, e.g., a skin-mode-like bound state inside the point-gap loop and anomalous quantum emitter dynamics without Hermitian counterparts [75].

In this work, we predict the unique photon-emitter dressed states and long-range emitter-emitter interaction by studying

a paradigm of photon-emitter interactions in a nonreciprocal Su-Schrieffer-Heeger (SSH) photonic chain. In addition to the existence of conventional chiral bound states and hidden bound states inside the line and point gaps, respectively, we unveil unusual chiral and extended photon-emitter dressed states without Hermitian counterparts. Moreover, we demonstrate the directional long-range emitter-emitter interaction mediated by dressed states, where the interaction range is limited only by the bath dissipation.

Model. We consider a set of N identical atoms, as quantum emitters, coupled to a 1D SSH photonic chain with L unit cells, as shown in Fig. 1. Each two-level atom, with ground state $|g\rangle$ and excited state $|e\rangle$, is coupled to each cavity in the lattice, and its decay rate is denoted by γ . The SSH photonic chain consists of coupled cavities subject to an engineered nonlocal photon dissipation between two sublattices a and b in each unit cell with loss rate κ . In the single-excitation subspace, the system dynamics is governed by the effective non-Hermitian Hamiltonian [see details for the nonlocal dissipation and effective non-Hermitian Hamiltonian in the Sec. I of the Supplemental Material (SM) [79]]

$$\begin{aligned} \hat{\mathcal{H}}_{\text{eff}} = & \sum_{n=1}^N \Delta \hat{\sigma}_n^+ \hat{\sigma}_n^- + \sum_{j=1}^{L-1} J_2 (\hat{a}_{j+1}^\dagger \hat{b}_j + \hat{b}_j^\dagger \hat{a}_{j+1}) \\ & + \sum_{j=1}^L \left[\left(J_1 + \frac{\kappa}{2} \right) \hat{b}_j^\dagger \hat{a}_j + \left(J_1 - \frac{\kappa}{2} \right) \hat{a}_j^\dagger \hat{b}_j \right] \\ & + \sum_{n=1}^N \sum_{\alpha \in \{a,b\}} \left[-i \frac{\kappa}{2} \hat{\alpha}_n^\dagger \hat{\alpha}_n + g (\hat{\alpha}_{j_n}^\dagger \hat{\sigma}_n^- + \text{H.c.}) \right], \quad (1) \end{aligned}$$

*These authors contributed equally to this work.

†Contact author: liutao0716@scut.edu.cn

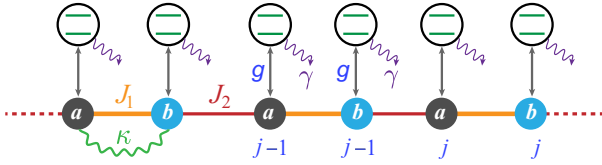


FIG. 1. Schematic showing a set of N identical two-level atoms (acting as quantum emitters) coupled to a 1D SSH photonic bath. The bath consists of coupled cavities, subject to correlated photon decay (with loss rate κ) between two cavities in each unit cell. J_1 and J_2 denote the intracell and intercell hopping strength, γ is the atomic decay rate, and g is the atom-photon coupling strength.

where $\hat{\sigma}_n^- = (\hat{\sigma}_n^+)^{\dagger} = |g_n\rangle\langle e_n|$ is the pseudospin ladder operator of the n th atom, $\Delta = \Delta_0 - i\gamma/2$ with frequency detuning Δ_0 , \hat{a}_j and \hat{b}_j annihilate photons at sublattices a and b of the j th unit cell (see Fig. 1), g is the photon-emitter interacting strength, and j_n labels the unit cell at which the n th atom is located. Unless otherwise specified, we assume $\gamma = \kappa$.

Chiral and hidden bound states. We couple a single emitter to the sublattice $\alpha \in \{a, b\}$ within the unit cell j_0 of the bath, and study the bound states lying within the regimes of both line and point gaps of the SSH bath. In the single-excitation subspace, the bound state using periodic boundary conditions (PBCs) can be written as $|\psi_b\rangle = [L^{-1/2} \sum_k (c_{k,a} \hat{a}_k^{\dagger} + c_{k,b} \hat{b}_k^{\dagger}) + c_e \hat{\sigma}_{j_0}^{\dagger}] |g\rangle \otimes |\text{vac}\rangle$, with $\hat{a}_k = L^{-1/2} \sum_j e^{-ikj} \hat{a}_j$ ($\alpha = a, b$), which satisfies $\hat{\mathcal{H}}_{\text{eff}}(k) |\psi_b\rangle = E_b |\psi_b\rangle$. For the photon-emitter bound states, we require $c_e \neq 0$. This yields [79]

$$\det[E_b - \Delta - \Sigma(E_b)] = 0, \quad (2)$$

where $\Sigma(z)$ is the atomic self-energy, given by

$$\Sigma(z) = \frac{1}{L} \sum_k g_k^{\dagger} (z - H_k)^{-1} g_k, \quad (3)$$

with the bath's Bloch Hamiltonian $H_k = -i\frac{\kappa}{2}\tau_0 + (J_1 + J_2 \cos k)\tau_x + (J_2 \sin k - i\kappa/2)\tau_y$, and $g_k = [g_a e^{-ikj_0}, g_b e^{-ikj_0}]^T$ ($g_a, g_b \in \{0, g\}$).

In the presence of line gap for $|J_2| < |J_1 - \kappa/2|$, we can analytically solve the real-space wave function of the bound state with $E_b = -i\kappa/2$ for $\Delta = -i\kappa/2$ [79]. For the emitter coupled to the sublattice a , we have $c_{j,a} = 0$, $c_{j,b} = -g c_e (-J_2)^{j-j_0} (J_1 - \kappa/2)^{-j+j_0-1}$ if $j \geq j_0$, and $c_{j,b} = 0$ if $j < j_0$. For the emitter coupled to the sublattice b , we have $c_{j,b} = 0$, $c_{j,a} = g c_e J_2^{j_0-j} (-J_1 - \kappa/2)^{j-j_0-1}$ if $j \leq j_0$, and $c_{j,a} = 0$ if $j > j_0$. These indicate that the bound state lying within the line gap [see red filled square marker in Fig. 2(a)] shows perfect chiral photon weight $|c_j|^2$ for $\Delta = -i\kappa/2$, as shown in Fig. 2(b1). Such a chiral bound state can be interpreted as a boundary between two semi-infinite chains with different topology [12], its chirality thus depends on the sublattice a or b which the emitter is coupled to, and is insensitive to the NHSE. Note that the chirality of the bound state is sensitive to Δ (see details in the Sec. III of the SM [79]).

As a comparison, we calculate the bound state lying inside the point gap, which can be analytically solved out for $J_1 = \kappa/2$ [79]. The self-energy of the bound state is obtained as

$$\Sigma(E_b) = \begin{cases} -\frac{g^2(E_b + \frac{i\kappa}{2})}{J_2^2 - (E_b + \frac{i\kappa}{2})^2}, & |\kappa J_2| < |J_2^2 - (E_b + i\kappa/2)^2| \\ 0, & |\kappa J_2| > |J_2^2 - (E_b + i\kappa/2)^2| \end{cases}. \quad (4)$$

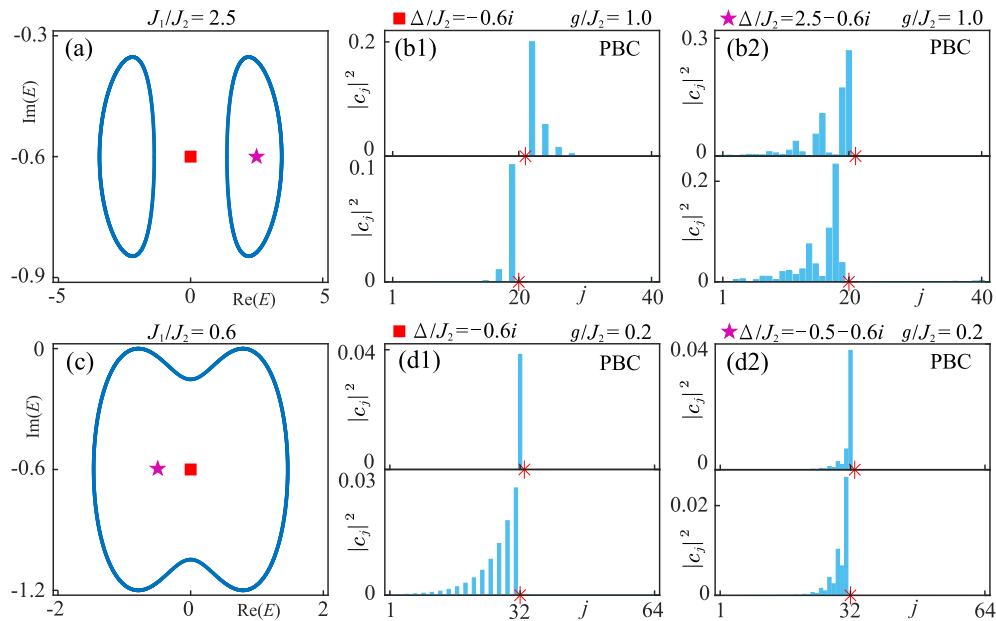


FIG. 2. Single-excitation spectrum (blue loops) under PBCs (a) with the coexistence of point and line gaps for $J_1/J_2 = 2.5$, and (c) with only a point gap for $J_1/J_2 = 0.6$. The markers denote the eigenenergies of the bound states of a single emitter coupled to the bath for different Δ/J_2 . The corresponding site-resolved photon weights $|c_j|^2$ are shown in (b1), (b2) and (d1), (d2), where the emitter is coupled to the sublattice a (b), denoted by the red asterisk, for the top (bottom) plot. The other parameters used are $\kappa/J_2 = 1.2$.

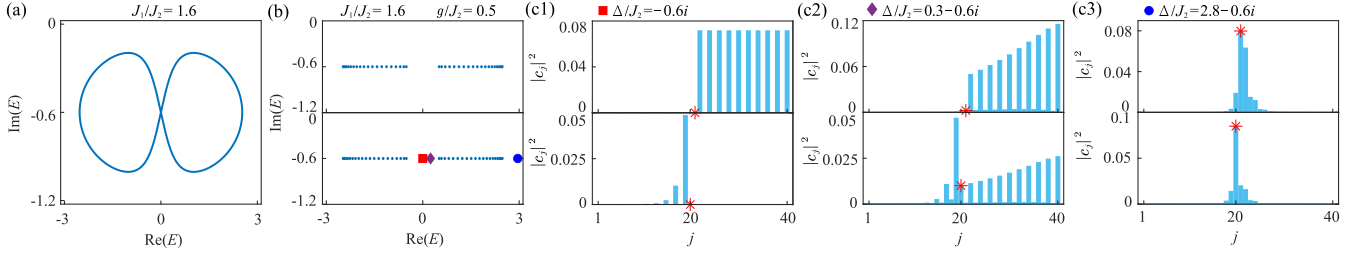


FIG. 3. Single-excitation spectrum of the SSH bath at transition point $J_2 = J_1 - \kappa/2$ under (a) PBCs and (b) OBCs (top plot). The markers, shown in bottom plot of (b), denote the eigenenergies of the dressed states of a single emitter coupled to the chain for different values of Δ/J_2 . The corresponding site-resolved photon weights $|c_j|^2$ are shown in (c1)–(c3) under OBCs, where the emitter is coupled to the sublattice a (b), denoted by the red asterisk, for the top (bottom) plot. The parameters used are $g/J_2 = 0.5$, $\kappa/J_2 = 1.2$, $J_1/J_2 = 1.6$, and $L = 20$.

The analytical results for the real-space wave functions are provided in the SM [79]. The self-energy in Eq. (4) vanishes for E_b lying inside the loop of the point gap, dubbed a hidden bound state [75]. In contrast to conventional bound states, such a bound state exhibits skin-mode-like localization independent of Δ [see Fig. 2(b2) and 2(c)–2(d2)], which is determined by the NHSE associated with the point-gap topology of the bath. Note that the emergence of hidden bound states does not rely on the coupling strength g (see details in Sec. III of the SM [79]).

Chiral-extended dressed states. In addition to localized chiral and hidden bound states, we identify a *unique in-gap photon-emitter dressed state*, exhibiting the chiral and extended mode distribution under OBCs. We consider the system parameter satisfying $J_2 = J_1 \pm \kappa/2$, where the line band gap closes (with the appearance of an exceptional point) under PBCs [see the PBC spectrum in Fig. 3(a)]. According to the non-Bloch bulk-boundary correspondence in a generalized Brillouin zone [79], the true topological-phase transition point of band topology is determined by $J_1 = \pm\sqrt{J_2^2 + (\kappa/2)^2}$. It is thus topologically trivial for $J_2 = J_1 - \kappa/2$ with $J_1 > \kappa/2$ [see OBC spectrum in the top plot of Fig. 3(b)]. Unless otherwise specified, we consider this condition for system parameters below.

We first study a single emitter coupled to the sublattice $\alpha \in \{a, b\}$ of the unit cell j_0 . In the single-excitation subspace under OBC, the photon-emitter dressed state is written as $|\psi_d\rangle = (\sum_{j,\alpha \in \{a,b\}} c_{j,\alpha} \hat{\alpha}_j^\dagger + c_e \hat{\sigma}^\dagger) |g\rangle \otimes |0\rangle$, which satisfies $\hat{\mathcal{H}}_{\text{eff}} |\psi_d\rangle = E_d |\psi_d\rangle$. Then we achieve

$$\Delta c_e + g c_{j_0, \alpha} = E_d c_e, \quad (5)$$

$$g c_e \delta_{j, j_0} \delta_{\alpha, a} + J_2 (c_{j, b} + c_{j-1, b}) = (E_d + i\kappa/2) c_{j, a}, \quad (6)$$

$$g c_e \delta_{j, j_0} \delta_{\alpha, b} + (J_2 + \kappa) c_{j, a} + J_2 c_{j+1, a} = (E_d + i\kappa/2) c_{j, b}. \quad (7)$$

For $\Delta = -i\kappa/2$, we can find the analytical solution for the dressed state with its eigenenergy $E_d = \Delta$. In this case, when the emitter is coupled to the sublattice a ($\alpha = a$) in Eqs. (5)–(7), we obtain $c_{j, a} = 0$, $c_{j, b} = 0$ for $j < j_0$, $c_e = -J_2 c_{j, b} / g$ for $j = j_0$, and $c_{j, b} = -c_{j-1, b}$ for $j > j_0$. The analytical results indicate that the in-gap photon-emitter dressed state exhibits an unconventional feature different from the one of the bound state when the emitter is coupled to the sublattice a . In addition to the chiral property with its eigenstate only

distributed on the right side of the emitter, the dressed state is uniformly distributed along the b sites under OBC, as shown in the top plot of Fig. 3(c1). [Its eigenenergy is indicated by the red square marker in the bottom plot of Fig. 3(b).] Noticeably, the chiral and extended photon-emitter dressed states are quite robust against the disordered-distributed cavity frequencies and disordered photonic hopping between cavities, as explained in Sec. IV of the SM [79].

In contrast, when the emitter is coupled to the sublattice b ($\alpha = b$) in Eqs. (5)–(7), we obtain $c_{j, b} = 0$, $c_{j-1, a} = -J_2 c_{j, a} / (J_2 + \kappa)$ for $j < j_0$, $c_e = -(J_2 + \kappa) c_{j, a} / g$ for $j = j_0$, and $c_{j, a} = 0$ for $j > j_0$. It turns out that the in-gap photon-emitter dressed state is bounded, and its photonic profile [see the bottom plot of Fig. 3(c1)] is localized at the left side of the emitter, i.e., showing the emergence of a chiral bound state.

The physical intuition of the appearance of the in-gap chiral and extended photon-emitter dressed states for $\Delta = -i\kappa/2$ with $J_2 = J_1 - \kappa/2$ can be attributed to the competition of topological-edge localization and non-Hermitian skin-mode localization with the combination of the non-Bloch bulk-boundary correspondence of a non-Hermitian topological bath. Namely, when the emitter is coupled to the sublattice a under OBC, we divide the photon-emitter system into two subsystems S_1 and S_2 , by breaking the intercell coupling $J_c = J_2$ that exists on the left side of the sublattice lattice a at the unit cell j_0 , as shown in Fig. 4. The subsystem S_1 is topologically trivial, while the subsystem S_2 hosts an in-gap topological edge mode where the emitter acts as the effective boundary of S_2 . Instead of topological-edge localization on the left side of the subsystem S_2 , the competition from the opposite mode localization towards the right side induced by NHSE leads to the extended mode distribution along the S_2 at $J_2 = J_1 - \kappa/2$ [80,81]. The coupling of the trivial subsystem S_1 to S_2 only has a minor effect on the dressed state due to

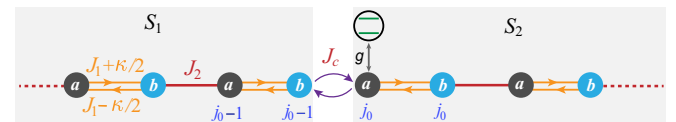


FIG. 4. Schematic for understanding the chiral and extended dressed state. When the emitter is coupled to the sublattice a under OBC, the hybrid system is divided into S_1 and S_2 subsystems by breaking the intercell coupling $J_c = J_2$ that exists on the left side of the sublattice lattice a at the unit cell j_0 .

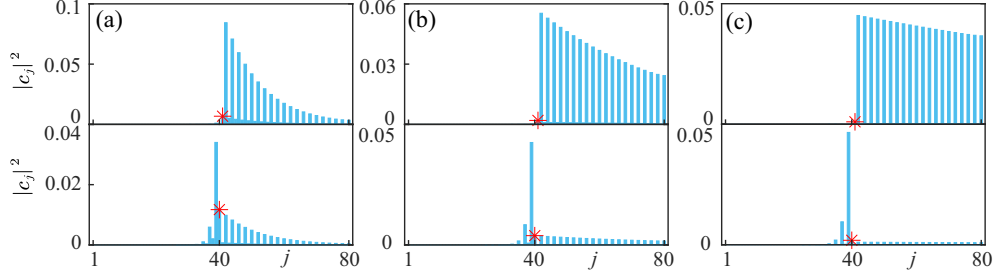


FIG. 5. Site-resolved photon weights $|c_j|^2$ at $J_2 = J_1 - \kappa/2$ for (a) $\gamma/J_2 = 0.4$, (b) $\gamma/J_2 = 0.8$, and (c) $\gamma/J_2 = 1.0$ under OBCs. The emitter is coupled to the sublattice a (b) for the top (bottom) plot. The other parameters used are $g/J_2 = 0.5$, $\kappa/J_2 = 1.2$, $J_1/J_2 = 1.6$, and $L = 40$.

its in-gap topological protection and zero occupations on a sublattices. Here the broken bulk-boundary correspondence of the topological bath due to NHSE excludes the coupling of the photon-emitter dressed state with the edge states of the SSH bath. However, when the emitter is coupled to the sublattice b , two subsystems S_1 and S_2 are constructed by breaking the intercell coupling $J_c = J_2$ that exists on the right side of the sublattice b at the unit cell ($j_0 - 1$). In this case, both topological edge-mode localization and NHSE lead to the formation of the chiral localized in-gap bound state.

For arbitrary Δ , we can still achieve the analytical solution of the eigenenergy $E_d = E - i\kappa/2$ for the dressed state [79], with E satisfying

$$E - \Delta_0 - g^2 \sum_{m=1}^{2L} \frac{|\varphi_{m,\alpha}(j_0)|^2}{(E - \varepsilon_m)\mathcal{N}_m} = 0, \quad (8)$$

where $\varepsilon_m = (-1)^m \sqrt{2\bar{J}_1 J_2 \cos \theta_m + \bar{J}_1^2 + J_2^2}$, with $\bar{J}_1 = \sqrt{(J_1 - \kappa/2)(J_1 + \kappa/2)}$, and real number θ_m , is the analytical eigenvalue of the non-Hermitian bath, and $\varphi_{m,\alpha}(j)$ ($\alpha = a, b$) is the element of the analytical eigenvectors of the Hermitian SSH lattice in the similarity-transformed basis with $\tilde{\mathcal{H}}_\alpha = S_\alpha^{-1} \mathcal{H}_\alpha S_\alpha$ (\mathcal{H}_α is the Hamiltonian matrix of $\hat{\mathcal{H}}_{\text{eff}}$ for the emitter coupled to the sublattice α , and S_α is the diagonal matrix $\text{diag}[1, r^{-(j_0 - \delta_{\alpha,a})}, r^{1 - (j_0 - \delta_{\alpha,a})}, \dots, r^{L - (j_0 - \delta_{\alpha,a})}]$ with $r = \sqrt{(J_1 + \kappa/2)/(J_1 - \kappa/2)}$ see details in Sec. V of the SM [79]), and \mathcal{N}_m is a normalization. This analytical result provides additional understanding of the chiral and extended dressed states for $\alpha = a$: in the similarity-transformed basis, the photon-emitter dressed state is bound with the photon weight power-law decaying towards the right side of the emitter [12]. After employing the inverse of the similarity transformation, the bound state becomes extended due to the power-law increase for each element of S_α starting at the site j_0 .

Figure 3(c2) shows the photon weight $|c_j|^2$ with $\Delta \neq -i\kappa/2$ for the emitter coupled to the sublattice $\alpha = a$ ($\alpha = b$) in the top (bottom) plot. The extended dressed states remain chiral with the uniform site-resolved photon weight for $\alpha = a$, while the bound state becomes extended distribution for $\alpha = b$. Note that there exist only bound states when the Δ is set to be outside the middle gap of the OBC spectrum [see Fig. 3(c3)].

Dissipation-controlled state profiles. We have discussed the chiral-extended photon-emitter dressed states for $\gamma = \kappa$. We now study the effects of the emitter decay rate γ on the mode

distribution of the dressed state with $\Delta_0 = 0$ and $J_2 = J_1 - \kappa/2$. As shown in Fig. 5, we show the site-resolved photon weights $|c_j|^2$ for the emitter coupled to the sublattice a (b) in the top (bottom) plot.

As discussed above, when the emitter is coupled to the sublattice a with $\gamma = \kappa$, an extended uniform distribution of chiral dressed states is achieved. This chiral-extended state distribution remains quite robust even when γ deviates from κ . As shown in top plots of Figs. 5(a)–5(c), the photon-emitter dressed states maintain chiral and extended distributions despite a significant deviation in emitter decay compared to cavity loss. Furthermore, as γ deviates from κ , the state distribution becomes nonuniform, with the photon weight gradually diminishing across the lattice sites. These indicate that the emitter dissipation can be utilized to control the wave function profiles of dressed states, and can also be employed to modulate interaction dynamics between two quantum emitters. In addition, when the emitter is coupled to the sublattice b , the wave-function profiles of bound states are great changed as γ deviates from κ [see bottom plots of Figs. 5(a)–5(c)].

Two emitters. We now consider the consequences of such dressed states when two quantum emitters are coupled to the bath with $J_2 = J_1 - \kappa/2$. The bound states can mediate the emitter-emitter interactions, giving rise to the exotic many-body phases [12]. The distance of two interacting emitters is determined by the localization length of the bound state, leading to short-range interactions. In contrast, the extended in-gap dressed state can mediate long-range interactions, and its chiral character causes the directional interactions between emitters.

In order to demonstrate such long-range interactions, we calculate the nonunitary real-time dynamics governed by $|\psi_t\rangle = e^{-i\hat{\mathcal{H}}_{\text{eff}}t} |\psi_0\rangle$ for two emitters (labeled as 1 and 2) coupled to sites j_{1,α_1} and j_{2,α_2} ($\alpha_1, \alpha_2 = a$ or b) of the bath with $j_{2,\alpha_2} > j_{1,\alpha_1}$, respectively. The initial state is chosen as one excited emitter $|e_1\rangle$ or $|e_2\rangle$ with $|\psi_0\rangle = |e_n\rangle |\text{vac}\rangle$ ($n = 1$ or 2), and the time-evolved state can be expanded as $|\psi_t\rangle = (\sum_{m=1}^{2N} c_m(t) |\varphi_m^R\rangle |\text{vac}\rangle + \sum_{n=1}^2 c_{e_n}(t) |e_n\rangle |g\rangle |gg\rangle \otimes |\text{vac}\rangle)$ ($|\varphi_m^R\rangle$ is the right eigenvector of the non-Hermitian bath). Using the resolvent method [82,83], we can express $\mathbf{c}_e(t) = [c_{e_1}(t), c_{e_2}(t)]^T$ as [79]

$$\mathbf{c}_e(t) = \frac{i}{2\pi} \int_{-\infty}^{+\infty} dE \mathcal{G}_p(E + i0^+) e^{-iEt} \mathbf{c}_e(0), \quad (9)$$

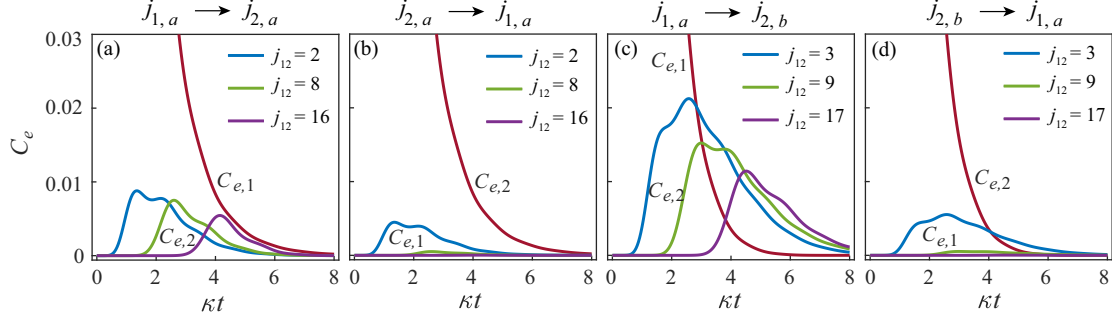


FIG. 6. Excited-state probability $C_{e,i} = |c_{e_i}(t)|^2$ ($i = 1, 2$) for two emitters coupled to sites j_{1,α_1} and j_{2,α_2} ($\alpha_1, \alpha_2 = a$ or b , and $j_{2,\alpha_2} > j_{1,\alpha_1}$) of the bath, where the emitter, coupled to the site $j_{1,a}$, $j_{2,a}$, $j_{1,a}$, and $j_{2,b}$, is initially excited for (a)–(d), respectively. The parameters used are $g/J_2 = 0.4$, $\kappa/J_2 = 0.4$, $J_1/J_2 = 1.2$, $\Delta/J_2 = -0.2i$, and $L = 100$.

where the Green's function $\mathcal{G}_p(z)$ is given by

$$\mathcal{G}_p(E) = \begin{pmatrix} \frac{1}{E - \Delta - \mathcal{T}(\alpha_1, \alpha_1)} & \frac{1}{E - \mathcal{F}(\alpha_1, \alpha_2)\mathcal{T}(\alpha_1, \alpha_2)} \\ \frac{1}{E - \mathcal{F}(\alpha_2, \alpha_1)\mathcal{T}(\alpha_1, \alpha_2)} & \frac{1}{E - \Delta - \mathcal{T}(\alpha_2, \alpha_2)} \end{pmatrix}, \quad (10)$$

with

$$\mathcal{T}(\alpha_1, \alpha_2) = g^2 \sum_{m=1}^{2L} \frac{\varphi_{m,\alpha_1}(j_{1,\alpha_1})\varphi_{m,\alpha_2}(j_{2,\alpha_2})}{(E - \varepsilon_m + i\kappa/2)\mathcal{N}_m}, \quad (11)$$

$$\mathcal{F}(\alpha_1, \alpha_2) = \frac{(J_1 + \kappa/2) \frac{j_{1,\alpha_1} - j_{2,\alpha_2} + \delta_{\alpha_1,b} - \delta_{\alpha_2,b}}{2}}{(J_1 - \kappa/2) \frac{j_{1,\alpha_1} - j_{2,\alpha_2} + \delta_{\alpha_1,b} - \delta_{\alpha_2,b}}{2}}. \quad (12)$$

According to Eqs. (9)–(12), the main contribution from the diagonal elements of the Green's function $\mathcal{G}_p(z)$ to the time evolution is the dressed state for small g and $\Delta = -i\kappa/2$. The off-diagonal elements contribute to the state exchanges between two emitters. Remarkably, such state exchange is asymmetrical [see Eq. (12)]. To be specific, when the emitter at the site j_{2,α_2} is initially excited, there is no excitation transferred to the emitter at the site j_{1,α_1} for the large distance $|j_{1,\alpha_1} - j_{2,\alpha_2}|$ between them due to the power-law decay of $\mathcal{F}(\alpha_1, \alpha_2)$. Figure 6 shows the excited-state probability $C_{e,i} = |c_{e_i}(t)|^2$ ($i = 1, 2$) for two emitters coupled to sites j_{1,α_1} and j_{2,α_2} of the bath, where the emitter, coupled to the site $j_{1,a}$, $j_{2,a}$, $j_{1,a}$, and $j_{2,b}$, is initially excited for Figs. 6(a)–6(d), respectively. When the first emitter coupled to the site $j_{1,a}$ is initially in the excited state, this will excite the second emitter at the $j_{2,a}$, even in a very large separation away from the first emitter [see Figs. 6(a) and 6(c)], which is limited by the intrinsic dissipation of the bath. In contrast, when the second emitter coupled to the site $j_{2,a}$ is initially in the excited state, no excitation is transferred to the first emitter at the site $j_{1,a}$ for a slight separation between them. The nonreciprocal long-range emitter-emitter interaction can induce exotic many-body phenomena, which is worth further investigation.

Conclusion and outlook. In summary, we have studied the conventional chiral and hidden bound states lying inside the line and point gaps of the 1D non-Hermitian topological bath, to which a single emitter is coupled. Most remarkably, we found a unique photon-emitter dressed state without Hermitian counterparts, showing the chiral and extended distribution on just one side of the emitter along the bath. Moreover, dissipation can shape the wave-function profile of the dressed state. The unconventional dressed states mediate the nonreciprocal long-range emitter-emitter interactions with the range limited by the bath dissipation. Our study opens many possible directions for future studies, e.g., exploring novel many-body phases of emergent spin models with long-range interactions of many emitters, peculiar extended dressed states in higher-dimensional non-Hermitian topological baths, and non-Markovian dynamics.

Acknowledgments. T.L. acknowledges the support from National Natural Science Foundation of China (Grant No. 12274142), the Key Program of the National Natural Science Foundation of China (Grant No. 62434009), the Introduced Innovative Team Project of the Guangdong Pearl River Talents Program (Grant No. 2021ZT09Z109), and the Startup Grant of the South China University of Technology (Grant No. 20210012). X.W. is supported by the National Natural Science Foundation of China (NSFC; Grants No. 12174303 and No. 11804270) and the Fundamental Research Funds for the Central Universities (Grant No. xzy012023053). F.N. is supported in part by the Japan Science and Technology Agency (JST) [via the Quantum Leap Flagship Program (Q-LEAP) and the Moonshot R&D Grant No. JPMJMS2061], the Asian Office of Aerospace Research and Development (AOARD) (via Grant No. FA2386-20-1-4069), and the Office of Naval Research (ONR) Global (via Grant No. N62909-23-1-2074).

Data availability. The data that support the findings of this article are not publicly available. The data are available from the authors upon reasonable request.

[1] A. González-Tudela and J. I. Cirac, Quantum emitters in two-dimensional structured reservoirs in the nonperturbative regime, *Phys. Rev. Lett.* **119**, 143602 (2017).

[2] A. González-Tudela and J. I. Cirac, Markovian and non-Markovian dynamics of quantum emitters coupled to two-dimensional structured reservoirs, *Phys. Rev. A* **96**, 043811 (2017).

- [3] P. Bienias, I. Boettcher, R. Belyansky, A. J. Kollár, and A. V. Gorshkov, Circuit quantum electrodynamics in hyperbolic space: From photon bound states to frustrated spin models, *Phys. Rev. Lett.* **128**, 013601 (2022).
- [4] A. F. Kockum, G. Johansson, and F. Nori, Decoherence-free interaction between giant atoms in waveguide quantum electrodynamics, *Phys. Rev. Lett.* **120**, 140404 (2018).
- [5] I. García-Elcano, A. González-Tudela, and J. Bravo-Abad, Tunable and robust long-range coherent interactions between quantum emitters mediated by Weyl bound states, *Phys. Rev. Lett.* **125**, 163602 (2020).
- [6] X. Wang, T. Liu, A. F. Kockum, H.-R. Li, and F. Nori, Tunable chiral bound states with giant atoms, *Phys. Rev. Lett.* **126**, 043602 (2021).
- [7] L. Leonforte, A. Carollo, and F. Ciccarello, Vacancy-like dressed states in topological waveguide QED, *Phys. Rev. Lett.* **126**, 063601 (2021).
- [8] D. De Bernardis, Z.-P. Cian, I. Carusotto, M. Hafezi, and P. Rabl, Light-matter interactions in synthetic magnetic fields: Landau-photon polaritons, *Phys. Rev. Lett.* **126**, 103603 (2021).
- [9] J. Perczel, J. Borregaard, D. E. Chang, H. Pichler, S. F. Yelin, P. Zoller, and M. D. Lukin, Topological quantum optics in two-dimensional atomic arrays, *Phys. Rev. Lett.* **119**, 023603 (2017).
- [10] R. J. Bettles, J. Minář, C. S. Adams, I. Lesanovsky, and B. Olmos, Topological properties of a dense atomic lattice gas, *Phys. Rev. A* **96**, 041603(R) (2017).
- [11] S. Barik, A. Karasahin, C. Flower, T. Cai, H. Miyake, W. DeGottardi, M. Hafezi, and E. Waks, A topological quantum optics interface, *Science* **359**, 666 (2018).
- [12] M. Bello, G. Platero, J. I. Cirac, and A. González-Tudela, Unconventional quantum optics in topological waveguide QED, *Sci. Adv.* **5**, eaaw0297 (2019).
- [13] E. Kim, X. Zhang, V. S. Ferreira, J. Banker, J. K. Iverson, A. Sipahigil, M. Bello, A. González-Tudela, M. Mirhosseini, and O. Painter, Quantum electrodynamics in a topological waveguide, *Phys. Rev. X* **11**, 011015 (2021).
- [14] C. Vega, M. Bello, D. Porras, and A. González-Tudela, Qubit-photon bound states in topological waveguides with long-range hoppings, *Phys. Rev. A* **104**, 053522 (2021).
- [15] C. Vega, D. Porras, and A. González-Tudela, Topological multimode waveguide QED, *Phys. Rev. Res.* **5**, 023031 (2023).
- [16] M. Bello, G. Platero, and A. González-Tudela, Spin many-body phases in standard- and topological-waveguide QED simulators, *PRX Quantum* **3**, 010336 (2022).
- [17] W. Nie, M. Antezza, Y.-x. Liu, and F. Nori, Dissipative topological phase transition with strong system-environment coupling, *Phys. Rev. Lett.* **127**, 250402 (2021).
- [18] D. E. Chang, J. S. Douglas, A. González-Tudela, C.-L. Hung, and H. J. Kimble, *Colloquium*: Quantum matter built from nanoscopic lattices of atoms and photons, *Rev. Mod. Phys.* **90**, 031002 (2018).
- [19] J.-S. Tang, W. Nie, L. Tang, M. Chen, X. Su, Y. Lu, F. Nori, and K. Xia, Nonreciprocal single-photon band structure, *Phys. Rev. Lett.* **128**, 203602 (2022).
- [20] A. S. Sheremet, M. I. Petrov, I. V. Iorsh, A. V. Poshakinskiy, and A. N. Poddubny, Waveguide quantum electrodynamics: Collective radiance and photon-photon correlations, *Rev. Mod. Phys.* **95**, 015002 (2023).
- [21] X. Wang, H.-B. Zhu, T. Liu, and F. Nori, Realizing quantum optics in structured environments with giant atoms, *Phys. Rev. Res.* **6**, 013279 (2024).
- [22] Z.-M. Gao, J.-Q. Li, Y.-H. Wu, W.-X. Liu, and X. Wang, Harnessing spontaneous emission of correlated photon pairs from ladder-type giant atoms, *Phys. Rev. A* **110**, 053706 (2024).
- [23] Z.-G. Lu, G. Tian, X.-Y. Lü, and C. Shang, Topological quantum batteries, *Phys. Rev. Lett.* **134**, 180401 (2025).
- [24] X. Wang, J.-Q. Li, T. Liu, A. Miranowicz, and F. Nori, Long-range four-body interactions in structured nonlinear photonic waveguides, *Phys. Rev. Res.* **6**, 043226 (2024).
- [25] A. González-Tudela, A. Reiserer, J. J. García-Ripoll, and F. J. García-Vidal, Light-matter interactions in quantum nanophotonic devices, *Nat. Rev. Phys.* **6**, 166 (2024).
- [26] X. Wang, J.-Q. Li, Z. Wang, A. F. Kockum, L. Du, T. Liu, and F. Nori, Nonlinear chiral quantum optics with giant-emitter pairs, [arXiv:2404.09829](https://arxiv.org/abs/2404.09829).
- [27] Y. Ashida, Z. Gong, and M. Ueda, Non-Hermitian physics, *Adv. Phys.* **69**, 249 (2020).
- [28] T. Gao, E. Estrecho, K. Y. Bliokh, T. C. H. Liew, M. D. Fraser, S. Brodbeck, M. Kamp, C. Schneider, S. Höfling, Y. Yamamoto, F. Nori, Y. S. Kivshar, A. G. Truscott, R. G. Dall, and E. A. Ostrovskaya, Observation of non-Hermitian degeneracies in a chaotic exciton-polariton billiard, *Nature (London)* **526**, 554 (2015).
- [29] F. Monifi, J. Zhang, Ş. K. Özdemir, B. Peng, Y.-x. Liu, F. Bo, F. Nori, and L. Yang, Optomechanically induced stochastic resonance and chaos transfer between optical fields, *Nat. Photon.* **10**, 399 (2016).
- [30] J. Zhang, B. Peng, Ş. K. Özdemir, K. Pichler, D. O. Krimer, G. Zhao, F. Nori, Y.-x. Liu, S. Rotter, and L. Yang, A phonon laser operating at an exceptional point, *Nat. Photon.* **12**, 479 (2018).
- [31] T. E. Lee, Anomalous edge state in a non-Hermitian lattice, *Phys. Rev. Lett.* **116**, 133903 (2016).
- [32] D. Leykam, K. Y. Bliokh, C. Huang, Y. D. Chong, and F. Nori, Edge modes, degeneracies, and topological numbers in non-Hermitian systems, *Phys. Rev. Lett.* **118**, 040401 (2017).
- [33] Y. Xu, S. T. Wang, and L. M. Duan, Weyl exceptional rings in a three-dimensional dissipative cold atomic gas, *Phys. Rev. Lett.* **118**, 045701 (2017).
- [34] Z. Gong, Y. Ashida, K. Kawabata, K. Takasan, S. Higashikawa, and M. Ueda, Topological phases of non-Hermitian systems, *Phys. Rev. X* **8**, 031079 (2018).
- [35] B. Peng, S. K. Özdemir, S. Rotter, H. Yilmaz, M. Liertzer, F. Monifi, C. M. Bender, F. Nori, and L. Yang, Loss-induced suppression and revival of lasing, *Science* **346**, 328 (2014).
- [36] R. El-Ganainy, K. G. Makris, M. Khajavikhan, Z. H. Musslimani, S. Rotter, and D. N. Christodoulides, Non-Hermitian physics and PT symmetry, *Nat. Phys.* **14**, 11 (2018).
- [37] S. Yao and Z. Wang, Edge states and topological invariants of non-Hermitian systems, *Phys. Rev. Lett.* **121**, 086803 (2018).
- [38] K. Zhang, Z. Yang, and C. Fang, Correspondence between winding numbers and skin modes in non-Hermitian systems, *Phys. Rev. Lett.* **125**, 126402 (2020).
- [39] K. Yokomizo and S. Murakami, Non-Bloch band theory of non-Hermitian systems, *Phys. Rev. Lett.* **123**, 066404 (2019).
- [40] S. Yao, F. Song, and Z. Wang, Non-Hermitian Chern bands, *Phys. Rev. Lett.* **121**, 136802 (2018).

- [41] F. K. Kunst, E. Edvardsson, J. C. Budich, and E. J. Bergholtz, Biorthogonal bulk-boundary correspondence in non-Hermitian systems, *Phys. Rev. Lett.* **121**, 026808 (2018).
- [42] T. Liu, Y.-R. Zhang, Q. Ai, Z. Gong, K. Kawabata, M. Ueda, and F. Nori, Second-order topological phases in non-Hermitian systems, *Phys. Rev. Lett.* **122**, 076801 (2019).
- [43] F. Song, S. Yao, and Z. Wang, Non-Hermitian skin effect and chiral damping in open quantum systems, *Phys. Rev. Lett.* **123**, 170401 (2019).
- [44] J. Y. Lee, J. Ahn, H. Zhou, and A. Vishwanath, Topological correspondence between Hermitian and non-Hermitian systems: Anomalous dynamics, *Phys. Rev. Lett.* **123**, 206404 (2019).
- [45] K. Kawabata, T. Bessho, and M. Sato, Classification of exceptional points and non-Hermitian topological semimetals, *Phys. Rev. Lett.* **123**, 066405 (2019).
- [46] W. Nie, T. Shi, Y.-x. Liu, and F. Nori, Non-Hermitian waveguide cavity QED with tunable atomic mirrors, *Phys. Rev. Lett.* **131**, 103602 (2023).
- [47] Z. Y. Ge, Y. R. Zhang, T. Liu, S. W. Li, H. Fan, and F. Nori, Topological band theory for non-Hermitian systems from the Dirac equation, *Phys. Rev. B* **100**, 054105 (2019).
- [48] H. Zhou and J. Y. Lee, Periodic table for topological bands with non-Hermitian symmetries, *Phys. Rev. B* **99**, 235112 (2019).
- [49] H. Zhao, X. Qiao, T. Wu, B. Midya, S. Longhi, and L. Feng, Non-Hermitian topological light steering, *Science* **365**, 1163 (2019).
- [50] K. Kawabata, K. Shiozaki, M. Ueda, and M. Sato, Symmetry and topology in non-Hermitian physics, *Phys. Rev. X* **9**, 041015 (2019).
- [51] D. S. Borgnia, A. J. Kruchkov, and R.-J. Slager, Non-Hermitian boundary modes and topology, *Phys. Rev. Lett.* **124**, 056802 (2020).
- [52] T. Liu, J. J. He, T. Yoshida, Z.-L. Xiang, and F. Nori, Non-Hermitian topological Mott insulators in one-dimensional fermionic superlattices, *Phys. Rev. B* **102**, 235151 (2020).
- [53] K. Y. Bliokh, D. Leykam, M. Lein, and F. Nori, Topological non-Hermitian origin of surface Maxwell waves, *Nat. Commun.* **10**, 580 (2019).
- [54] K. Yokomizo and S. Murakami, Scaling rule for the critical non-Hermitian skin effect, *Phys. Rev. B* **104**, 165117 (2021).
- [55] N. Okuma, K. Kawabata, K. Shiozaki, and M. Sato, Topological origin of non-Hermitian skin effects, *Phys. Rev. Lett.* **124**, 086801 (2020).
- [56] Y. Yi and Z. Yang, Non-Hermitian skin modes induced by on-site dissipations and chiral tunneling effect, *Phys. Rev. Lett.* **125**, 186802 (2020).
- [57] T. Liu, J. J. He, Z. Yang, and F. Nori, Higher-order Weyl-exceptional-ring semimetals, *Phys. Rev. Lett.* **127**, 196801 (2021).
- [58] E. J. Bergholtz, J. C. Budich, and F. K. Kunst, Exceptional topology of non-Hermitian systems, *Rev. Mod. Phys.* **93**, 015005 (2021).
- [59] Y. Li, C. Liang, C. Wang, C. Lu, and Y.-C. Liu, Gain-loss-induced hybrid skin-topological effect, *Phys. Rev. Lett.* **128**, 223903 (2022).
- [60] C. Leefmans, A. Dutt, J. Williams, L. Yuan, M. Parto, F. Nori, S. Fan, and A. Marandi, Topological dissipation in a time-multiplexed photonic resonator network, *Nat. Phys.* **18**, 442 (2022).
- [61] K. Zhang, Z. Yang, and C. Fang, Universal non-Hermitian skin effect in two and higher dimensions, *Nat. Commun.* **13**, 2496 (2022).
- [62] M. Parto, C. Leefmans, J. Williams, F. Nori, and A. Marandi, Non-Abelian effects in dissipative photonic topological lattices, *Nat. Commun.* **14**, 1440 (2023).
- [63] Z. Ren, D. Liu, E. Zhao, C. He, K. K. Pak, J. Li, and G.-B. Jo, Chiral control of quantum states in non-Hermitian spin-orbit-coupled fermions, *Nat. Phys.* **18**, 385 (2022).
- [64] K. Kawabata, T. Numasawa, and S. Ryu, Entanglement phase transition induced by the non-Hermitian skin effect, *Phys. Rev. X* **13**, 021007 (2023).
- [65] K. Zhang, C. Fang, and Z. Yang, Dynamical degeneracy splitting and directional invisibility in non-Hermitian systems, *Phys. Rev. Lett.* **131**, 036402 (2023).
- [66] C.-A. Li, B. Trauzettel, T. Neupert, and S.-B. Zhang, Enhancement of second-order non-Hermitian skin effect by magnetic fields, *Phys. Rev. Lett.* **131**, 116601 (2023).
- [67] W.-W. Jin, J. Liu, X. Wang, Y.-R. Zhang, X. Huang, X. Wei, W. Ju, T. Liu, Z. Yang, and F. Nori, Reentrant non-Hermitian skin effect induced by correlated disorder, [arXiv:2311.03777](https://arxiv.org/abs/2311.03777).
- [68] Z.-F. Cai, T. Liu, and Z. Yang, Non-Hermitian skin effect in periodically driven dissipative ultracold atoms, *Phys. Rev. A* **109**, 063329 (2024).
- [69] X. Li, J. Liu, and T. Liu, Localization-delocalization transitions in non-Hermitian Aharonov-Bohm cages, *Front. Phys.* **19**, 33211 (2024).
- [70] H.-Y. Wang, F. Song, and Z. Wang, Amoeba formulation of non-Bloch band theory in arbitrary dimensions, *Phys. Rev. X* **14**, 021011 (2024).
- [71] Y.-M. Hu, H.-Y. Wang, Z. Wang, and F. Song, Geometric origin of non-Bloch \mathcal{PT} symmetry breaking, *Phys. Rev. Lett.* **132**, 050402 (2024).
- [72] C. R. Leefmans, M. Parto, J. Williams, G. H. Y. Li, A. Dutt, F. Nori, and A. Marandi, Topological temporally mode-locked laser, *Nat. Phys.* **20**, 852 (2024).
- [73] F. Roccati, S. Lorenzo, G. Calajò, G. M. Palma, A. Carollo, and F. Ciccarello, Exotic interactions mediated by a non-Hermitian photonic bath, *Optica* **9**, 565 (2022).
- [74] Z. Gong, M. Bello, D. Malz, and F. K. Kunst, Bound states and photon emission in non-Hermitian nanophotonics, *Phys. Rev. A* **106**, 053517 (2022).
- [75] Z. Gong, M. Bello, D. Malz, and F. K. Kunst, Anomalous behaviors of quantum emitters in non-Hermitian baths, *Phys. Rev. Lett.* **129**, 223601 (2022).
- [76] L. Du, L. Guo, Y. Zhang, and A. F. Kockum, Giant emitters in a structured bath with non-Hermitian skin effect, *Phys. Rev. Res.* **5**, L042040 (2023).
- [77] F. Roccati, M. Bello, Z. Gong, M. Ueda, F. Ciccarello, A. Chenu, and A. Carollo, Hermitian and non-Hermitian topology from photon-mediated interactions, *Nat. Commun.* **15**, 2400 (2024).
- [78] D. A. Lidar, Lecture notes on the theory of open quantum systems, [arXiv:1902.00967](https://arxiv.org/abs/1902.00967).
- [79] See Supplemental Material at <http://link.aps.org/supplemental/10.1103/8qpx-68x6> for (I) effective non-Hermitian bath in single-excitation subspace, (II) bulk-boundary correspondence of a non-Hermitian SSH bath, (III) chiral and hidden bound

- states, (IV) effects of disorder on chiral and extended photon-emitter dressed states, and (V) analytical solution of chiral-extended photon-emitter dressed states, which includes Refs. [84–88].
- [80] W. Zhu, W. X. Teo, L. Li, and J. Gong, Delocalization of topological edge states, *Phys. Rev. B* **103**, 195414 (2021).
- [81] W. Wang, X. Wang, and G. Ma, Non-Hermitian morphing of topological modes, *Nature (London)* **608**, 50 (2022).
- [82] C. Cohen-Tannoudji, J. Dupont-Roc, and G. Grynberg, *Atom-Photon Interactions: Basic Process and Applications* (John Wiley and Sons, New York, 1998).
- [83] E. N. Economou, *Green's Functions in Quantum Physics* (Springer, Berlin, 2006).
- [84] M. O. Scully and M. S. Zubairy, *Quantum Optics* (Cambridge University Press, Cambridge, 1997).
- [85] H. P. Breuer and F. Petruccione, *The Theory of Open Quantum Systems* (Oxford University Press, Oxford, 2007).
- [86] Q. Liang, D. Xie, Z. Dong, H. Li, H. Li, B. Gadway, W. Yi, and B. Yan, Dynamic signatures of non-Hermitian skin effect and topology in ultracold atoms, *Phys. Rev. Lett.* **129**, 070401 (2022).
- [87] Z. Gong, S. Higashikawa, and M. Ueda, Zeno Hall effect, *Phys. Rev. Lett.* **118**, 200401 (2017).
- [88] C.-X. Guo, C.-H. Liu, X.-M. Zhao, Y. Liu, and S. Chen, Exact solution of non-Hermitian systems with generalized boundary conditions: Size-dependent boundary effect and fragility of the skin effect, *Phys. Rev. Lett.* **127**, 116801 (2021).